MINERALOGICAL MAGAZINE, DECEMBER 1983, VOL. 47, PP. 507-14.

Some aspects of the silver mineralization in the Hällefors region (Bergslagen, Sweden)

A. W. JASINSKI

Institute of Earth Sciences, Free University, De Boelelaan 1085, 1007 MC Amsterdam, The Netherlands

ABSTRACT. Sulphide and sulphosalt mineralization in the Hällefors silver mining district occurs as stratabound bodies in skarn-like black carbonates and other carbonates in the eastern part of the district, and as epigenetic, tectonically controlled vein mineralization in tuffaceous metavolcanics and, to a lesser extent in slates, in the western part.

Previous work has suggested that the Ag-bearing Hällefors deposits were formed by the action of metamorphic solutions on sediments of volcano-sedimentary origin. At the stages of sulphosalt and sulphide formation, temperature and pressure conditions were probably in the ranges 500–440 K and 4.5–3.5 kbar. Examination of a $\log a_{S_2}$–$1/T$ diagram and of Ag–Sb phase relations combined with study of the ores suggest the paragenesis of the Ag-bearing minerals is as follows: allargentum and dyscrasite as exsolution bodies in silver bearing galena; Ag-containing tetrahedrite → freibergite → miargyrite → pyrargyrite → stephanite (from hydrothermal solutions).

Geological setting and mineralization. The Hällefors silver deposits are located in the Bergslagen mining district which is in the northern part of the Grythyttan–Hällefors complex of the Central Swedish Svecofenides. The central zone of the complex consists of slates, conglomerates and graywackes, and the eastern part of ore-bearing leptite-like hälleflintas [rocks with conchoidal fracture, without visible granularity in the main mass although with well-defined phenocrysts of quartz and feldspar, and of ages determined as 1830 ± 50 Ma (Moorman *et al.*, 1982) or 1862 Ma (Welin *et al.*, 1980)]. The hälleflintas have intercalations of carbonate rocks (up to 150 m thick) and greenstones. Rocks of the Grythyttan–Hällefors area were affected by low-grade metamorphism of the greenschist facies (Sundius, 1923) during early Rift Stage folding of the BlackSlate–Tuffite–Siltstone–Greywacke Formation, which is younger than the hälleflintas (Oen *et al.*, 1982). The mineralization occurs in an area (2.5×1 km) situated 8 km north of Hällefors village (about 210 km WNW of Stockholm) and can be itself split into eastern and western parts (fig. 1).

In the eastern part, bordering the Silverknuten granite, hälleflinta, limestone and magnetite-bearing carbonate rocks occur with sulphide impregnations mainly along contacts and faults in the latter. The limestone here varies from pure white to darker yellow-white in colour. Within the limestone, strongly microfolded bands of hälleflinta are a normal phenomenon. An interesting assemblage here is made up of carbonates containing magnetite, olivine (knebelite), Fe–Mn carbonates with general formulae $Mn_{0.60}Fe_{0.21}Mg_{0.13}Ca_{0.06}CO_3$ (Sundius, 1923; Sundius *et al.*, 1966), clinoamphibole (from the cummingtonite–grünerite series, Sundius *et al.*, 1966), garnet ($Sp_{70}Alm_{19}An_9Py_2$, Sundius *et al.*, 1966), chlorites, micas, and serpentine.

The western part of the deposit, along with the more centrally located Mellan sector, consists of hälleflintas or of fine-grained slates (with crystals of quartz, mica, epidote and carbonate minerals); here the mineralization infills fissures in hälleflintas and also in slates and in minor bodies of greenstone. Contacts between these rocks and veins are often very sharp, although along the contacts there are the products of alteration caused by hydrothermal solutions. There are no skarn and carbonate rocks (Nugteren, 1978). Detailed descriptions of all these rocks are to be found in Sundius (1923).

The Bergslagen geochemical province is known as an important producer of Fe, Zn, Pb, Ag, Cu, and to a lesser extent of Mn, Co, W, Mo, Au, Bi, Ce, Hg, and Se (Tegengren, 1924). Regional mineralogical studies carried out at the Free University in Amsterdam point to a separation of Cu-bearing deposits (with associated minerals of Zn, Bi, Co, Mo, As, Au, Se, Te) from Pb–Zn–Ag deposits (with associated minerals of Sb, Mn, As, Sn, Cu, Hg). The Hällefors mines are members of the second group of deposits which are characterized by a high Pb/Cu ratio, lack of Bi and presence of As almost wholly confined to high-temperature arsenopyrite.

The major sulphide minerals in these deposits are arsenopyrite, sphalerite and galena. Besides these minerals, pyrrhotine, chalcopyrite and marcasite

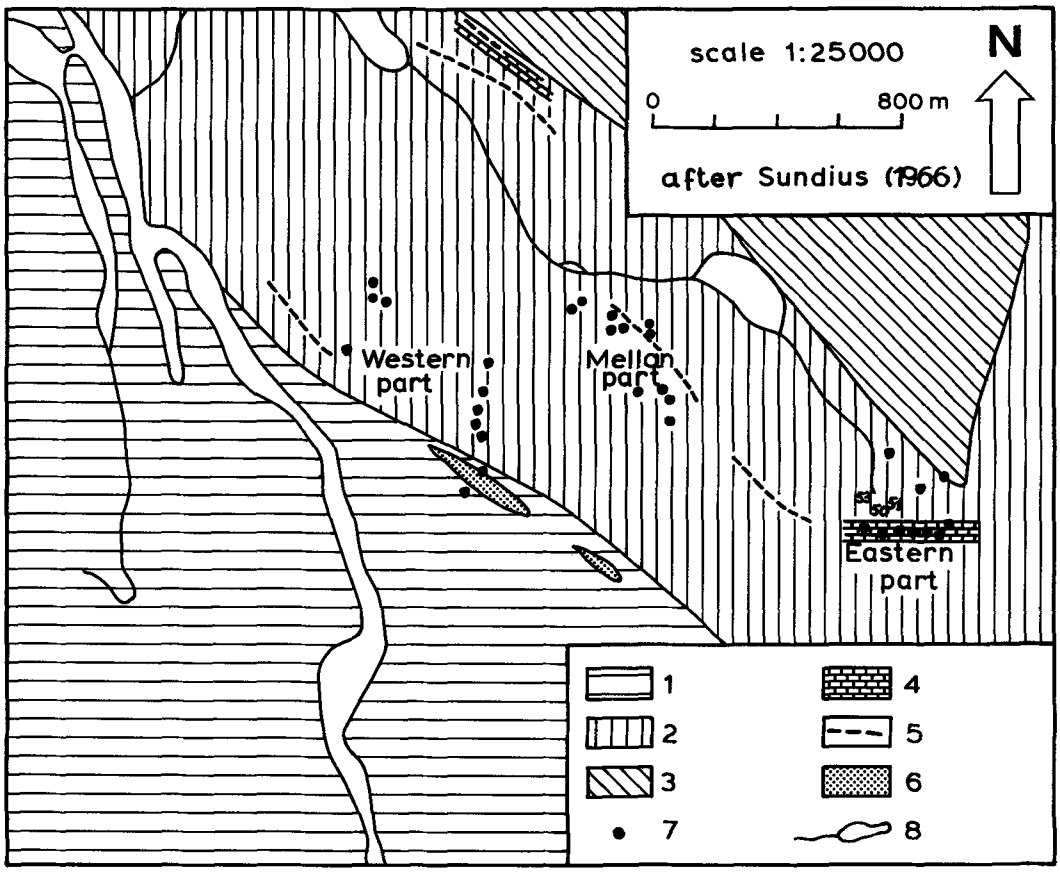

FIG. 1. The silver mines of Hällefors: 1, slate; 2, hälleflinta; 3, granophyric granite; 4, limestone; 5, greenstone dyke; 6, amygdaloid effusive greenstone; 7, silver mine; 8, lakes and rivers. 50, 51, 53 schematic locations of boreholes BH-50, BH-51, BH-53.

are common. Locally, pyrite, boulangerite, bournonite, meneghinite, gudmundite, and silver minerals are found. There are rare occurrences of native Sb, stibnite and stannite. Other minerals reported include magnetite, rutile, ilmenite, goethite, cassiterite, hematite, covellite, azurite, and malachite (Nugteren, 1978; Nugteren and Zakrzewski, in prep.; Sundius *et al.*, 1966). The Ag content of the ores is locally high; up to 1000 g/t Ag is present in galena (up to 0.3%) and also in Ag-bearing minerals (the most important of which are tetrahedrite, freibergite, pyrargyrite, miargyrite, and stephanite). Microscope observations indicate that in Ag-rich galena and to a lesser extent in gudmundite, allargentum, and dyscrasite occur. The most Ag-rich minerals, from the tetrahedrite-freibergite group, were found in the western sector of the deposit. Miargyrite, in association with pyrrhotine, chalcopyrite, freibergite and sphalerite, occurs in boulangerite-rich ores from the western mines. Pyrargyrite was found chiefly as inclusions in galena. Stephanite was noticed in the western part of the eastern sector as fracture fillings in galena and sphalerite (Nugteren and Zakrzewski, in prep.). Nugteren (1978) noted small Ag-Sb-bearing phases in galena, too small to be examined even by means of electron probe microanalysis. A typical paragenetic sequence determined for this area, beginning from pyrrhotine formation, is as follows: (pyrrhotine, chalcopyrite) → sphalerite → (galena, gudmundite?, tetrahedrite) → allargentum → (boulangerite, bournonite) → (pyrargyrite, native Sb, Ag-Sb-sulphosalts) → (marcasite, pyrite, hematite, covellite). Before pyrrhotine, according to Nugteren (1978), arsenopyrite and some of the pyrite, galena and sphalerite were precipitated.

Samples of these ores were chemically analysed by Boliden Metal AB; microscope, X-ray and electron probe studies have been undertaken by Nugteren and Zakrzewski (in prep.). Temperatures

of ore formation which are used in the calculations described below are from preliminary studies of two- and three-phase fluid inclusions in vein minerals of this deposit. Temperatures of homogenization of inclusions in quartz and sphalerite grains, determined by Coolen (pers. comm., 1981), are in the range 540–440 K. Rough estimation of pressures of ore formation have been made by Nugteren (pers. comm., 1981), using the sphalerite geobarometer. They have been determined as less than 6 kbar with values decreasing westwards.

Thermodynamic calculations. Thermodynamic calculations were undertaken using the data of Robie *et al.* (1978), Craig and Barton (1973). ΔG_r and $\log a_{S_2}$ were calculated from: $\Delta G_r = \Delta H_r - T\Delta S_r + \Delta V_{s,r}(P-1)$; $\log a_{S_2} = (A/T) + B + C(P-1)/T$, where $\Delta V_{s,r}$ = volume change of solid components of reaction (molar volumes were calculated from cell parameters taken from Kostov and Minceva-Stefanova, 1981). In ΔG equations for sulphosalts, the coefficient n (in the mixing entropy term $S_{mix} = -nR\Sigma N_i \ln N_i$) was assumed to have the following values:

(1) the Ag–Sb–S (pyrargyrite) system and polybasite, $n = 0.97$ (recalculated from ΔG_f of miargyrite).
(2) the (Cu,Ag)-(Fe,Zn)-Sb–S system, $n = 1$.
(3) the Ag–Pb–Sb–S system, $n = 0.97$.
(4) the Pb–Sb–S system (boulangerite), $n = 0.8$.

Table I shows the equations and the thermodynamic data employed in constructing fig. 2. The choice of coefficients was dictated both by microscopic investigations of mutual mineral relations and by the equations giving ΔG_f for sulphosalts calculated using the experimental values of Craig and Lees (1972). Thus, the tetrahedrite line calculated assuming $n = 1$ (473 K) lies below the limit of water–fluid stability and a tentatively calculated, but not presented here, line for meneghinite ($CuPb_{13}Sb_7S_{24}$; $n = 0.8$; 473 K; Jasinski, in prep.) lies just above it. For miargyrite and stephanite, the experimentally determined ΔG_f equations were used (Craig and Barton, 1973). Values used for n are in agreement with those proposed by these authors ($n = 1.2 \pm 0.8$) and the enthalpy of mixing was assumed to be zero.

Invariability of solid reagent volumes with temperature and an activity = 1 for all solid phases were also assumed in the calculations. In the $\log a_{S_2} - 1/T$ diagram (fig. 2), the line illustrating the lower limit of water fluid stability was calculated assuming a possible fluid composition with mole fractions $x_{CO_2} = 0.3$, $x_{H_2O} = 0.7$ which are in agreement with measurements of freezing temperature carried out by Coolen (pers. comm., 1981) and fugacity coefficients for 503 K, 4.5 kbar and 477 K, 4 kbar taken from Powell (1978). In calculations and reactions the mineral formulae listed in Table I have been used. Using the $Cu_{10}Fe_2Sb_4S_{13}$ formula for tetrahedrite (similar to the electron probe analysis of tetrahedrite from Berglundsgruvorna—the closest part of these deposits to the Silverknuten granite—Nugteren, 1978; Nugteren and Zakrzewski, in prep.) the reaction 8 is characterized by the lowest value of $\log a_{S_2}$. Other compositions for this mineral would give higher values of $\log a_{S_2}$. The formula used for freibergite ($Ag_6Cu_4Fe_{1.5}Zn_{0.5}Sb_4S_{13}$) allows the line (reaction 9) for this mineral to be located higher on the $\log a_{S_2} - 1/T$ diagram; for freibergite which is richer in silver, this line is displaced towards even higher values of $\log a_{S_2}$. Allowing for Cu in the formula of polybasite (reaction 10) causes a shift of this tenth line below the limit of freieslebenite stability. The pressure gradients assumed in the calculations were 500 bar/70 K (573–503 K) and 500 bar/30 K (503–443 K) although it is stressed that the influence of pressure on $\log a_{S_2}$ values is much lower than that of temperature.

Discussion. Study of Ag-bearing galena in these deposits suggests that Ag and Sb occur by isomorphic substitution in this mineral (up to 0.3%; Amcoff, 1976; Hall and Czamanske, 1972) and that allargentum (Ag_4Sb–Ag_8Sb) and dyscrasite occur by exsolution in galena. These observations are confirmed by study of the Ag–Sb phase diagram (Petruk *et al.*, 1971). Below 831 K, exsolution of the ε-phase (allargentum) and dyscrasite from a primary Ag–Sb solid solution is possible. The presence of Sb is favourable for Ag solubility in galena and it suggests $Ag^+ + Sb^{3+} \rightleftharpoons 2Pb^{2+}$ substitution and eventual formation of separate phases from the Pb–Ag–Sb–S system. Up to now there has been no evidence for the existence of the above-mentioned phases in the rocks studied. Gudmundite analysis gives Fe:Sb:S = 1:1:1 without Ag, Zn, or As (Nugteren, 1978; Nugteren and Zakrzewski, in prep.). However, coexistence of FeSbS with allargentum and simultaneous absence of galena point to gudmundite as a source of allargentum, perhaps as a result of the reaction: $(Fe,Ag)Sb_{(1+x)}S \rightarrow FeSbS + x\ Ag_6Sb$. This reaction could relate to the formation of Ag-bearing tetrahedrite in rims between gudmundite and chalcopyrite, for example, from the reaction: $40\ FeAg_{0.05}Sb_{1.0083}S + 8Cu FeS_2 + 9.668\ Sb + 3/2\ S_2 \rightarrow Cu_8Ag_2Fe_2Sb_4S_{13} + 46\ FeSbS$. An approximate determination of ΔG_r gives a negative value indicating that this reaction could run from left to right.

To determine a mechanism of deposit formation, especially for the sulphosalts, a $\log a_{S_2} - 1/T$ diagram was used (fig. 2). In this diagram, the path showing probable changes in the chemistry of

Table I Thermodynamical data and results of calculations

line	reaction, ΔG formation (ΔGf), ΔG reaction (ΔGr), log a_{s2}	n_{mix}	Calc. ΔS^{o}form. (cal) (for 298 K)
1	$2FeS + S_2 = 2FeS_2$ $\Delta Gr = -64450 + 58,07T + 0,278\ (P-1)$		
	$\log a_{s2} = -14084/T + 12,69 + 0,061\ (P-1)/T$		
2	$4/3\ Sb + S_2 = 2/3\ Sb_2S_3$ $\Delta Gr = -55430 + 40,10T + 0,59\ (P-1)$		
	$\log a_{s2} = -12113/T + 8,76 + 0,13\ (p-1)/T$		
3	$2/3\ FeSbS + 2/3\ Sb + S_2 = 2/3\ FeSb_2S_4$ $\Delta Gr = -57497 + 40,16T + 0,671\ (P-1)$		
	$\log a_{s2} = -12565/T + 8,77 + 0,146\ (P-1)/T$		
4	$5/3\ PbS + 4/3Sb + S_2 = 1/3\ Pb_5Sb_4S_{11}$ $\Delta Gr = -184834 - 21,96\ T$	0,8	226,55
	$\Delta Gr = -55430 + 36,09T + 0,059\ (P-1)$ $\log a_{s2} = -12113/T + 7,89 + 0,13\ (P-1)/T$		
5	$Ag + Sb + S_2 = AgSbS_2$ $\Delta G_f = -22063 - 7,33T$		
	$\Delta Gr = -52773 + 32,04T + 0,64\ (P-1)$ $\log a_{s2} = -11533/T + 7,0 + 0,14\ (p-1)/T$	0,97	
6	$2Ag + 2/3Sb + S_2 = 2/3\ Ag_3SbS_3$ $\Delta G_f = -26992 - 20,54T$		
	$\Delta Gr = -49449 + 25,63T + 0,7\ (P-1)$ $\log a_{s2} = -10806/T + 5,6 + 0,15\ (P-1)/T$	0,97	84,73
7	$5/3\ Ag + 1/2\ Sb + S_2 = 1/2\ Ag_5SbS_4$ $\Delta G_f = -36153 - 29,44T$		
	$\Delta Gr = -48786 + 24,61T + 0,67\ (P-1)$ $\log a_{s2} = -10661/T + 5,38 + 0,146\ (P-1)/T$		
	$2Ag + 0,4Sb_2S_3 + S_2 = 0,4\ Ag_5SbS_4$ $\Delta Gr = -5771 - 4,37T + 0,388\ (P-1)$		
	$\log a_{s2} = -1261/T - 0,95 + 0,085\ (P-1)/T$		
8	$5/3\ Cu_2S + 2/3\ FeS + 4/3\ Sb + S_2 = 1/3\ Cu_{10}Fe_2Sb_4S_{13}$ $\Delta G_f = -197795 - 96,42T$	1	330,98
	$\Delta Gr = -55430 + 31,38T + 0,7\ (P-1)$ $\log a_{s2} = -12113/T + 6,86 + 0,153\ (P-1)/T$		
9	$0,44\ Cu_2S + 1,333\ Ag + 0.333\ FeS + 0,111\ ZnS + 0,889Sb + S_2 =$		
	$= 0,222\ Cu_4Ag_6Fe_{1,5}Zn_{0,5}Sb_4S_{13}$	1	348,95
	$\Delta G_f = -177880 - 99,18T$ $\Delta Gr = -50896 + 24,42T + 0,64\ (P-1)$		
	$\log a_{s2} = -11122/T + 5,34 + 0,14\ (P-1)/T$		
10	$16Ag + 2Sb + 11/2\ S_2 = Ag_{16}Sb_2S_{11}$ $\Delta G_f = -82160 - 102,51T$	0,97	370,59
	$\Delta Gr = -251065 + 113,80T - 0,54\ (P-1)$ $\log a_{s2} = -9975/T + 4,52 - 0,022\ (P-1)/T$		
11	$Ag + PbS + Sb + S_2 = AgPbSbS_3$ $\Delta G_f = -43492 - 13,38T$	0,97	72,78
	$\Delta Gr = -52067 + 28,37T + 0,62\ (P-1)$ $\log a_{s2} = -11378/T + 6,20 + 0,135\ (P-1)/T$		
12	$Ag + 2/3\ PbS + Sb + S_2 = 1/3\ Ag_3Pb_2Sb_3S_8$ $\Delta G_f = -108342 - 35,41T$	0,97	190,46
	$\Delta Gr = -52068 + 29,15T + 0,62\ (P-1)$ $\log a_{s2} = -11378/T + 6,37 + 0,135\ (P-1)/T$		
13	$0,4Ag + 0,4\ PbS + 1,2\ Sb + S_2 = 0,4\ AgPbSb_3S_6$	0,97	108,54
	$\Delta Gr = -54085 + 34,40T + 0,60\ (P-1)$ $\log a_{s2} = -11819/T + 7,52 + 0,13\ (P-1)/T$		
14(A)	$1/2\ O_2 + H_2 = H_2O$ $0 = \Delta G^{o}_{1,298} + F_{H_2O} + RT \ln a_{H_2O} + RT \ln a_{H_2O} - \frac{1}{2} RT \ln ao_2$ $-RT \ln aH_2$		
	473 K, 4kba $F_{H_2O} = -7935 + 2615T$ $RT \ln \gamma_{H_2O} = (4971 - 35,85T).\ X^2_{co_2}$		
	503 K, 4,5 kba $F_{H_2O} = -7798 + 26,29T$		
14(B)	$3\ FeS + 2\ O_2 = Fe_3O_4 + 3/2\ S_2$ $\Delta G_r = -148210 + 24,5T - 0,241\ (P-1)$		
	$\log a_{s2} = 21592/T - 3,58 + 1,333 \log a_{O_2} + 0,035\ (P-1)/T$		

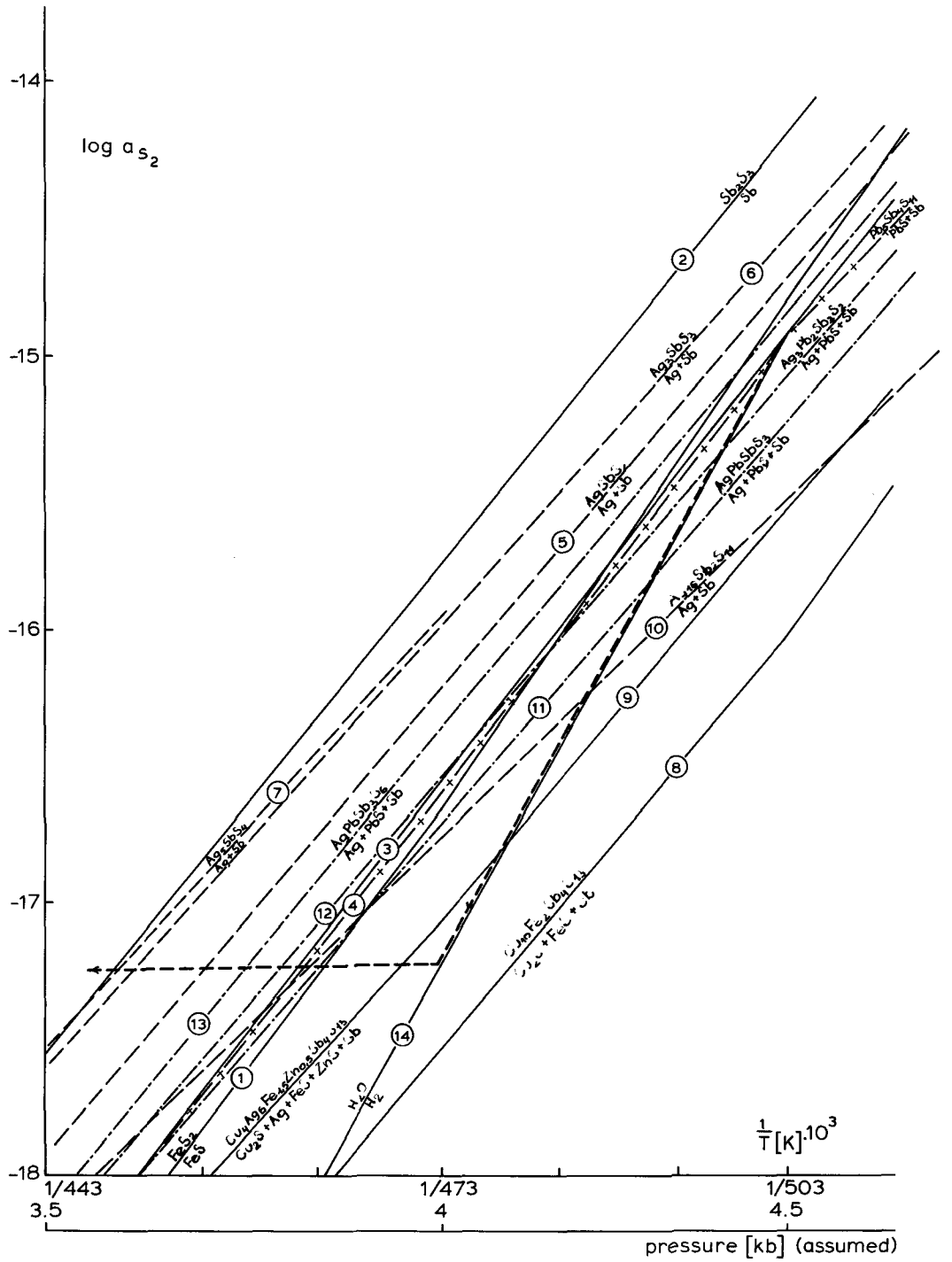

FIG. 2. Log $a_{S_2} - 1/T$ diagram. Arrowed dashed line represents path of probable changes in the chemistry of metal-bearing fluids. Numbers represent stability limits for: 1, pyrrhotine, pyrite; 2, stibnite; 3, gudmundite/berthierite; 4, boulangerite; 5, miargyrite; 6, pyrargyrite; 7, stephanite; 8, tetrahedrite; 9, freibergite; 10, polybasite; 11, freieslebenite; 12, diaphorite; 13, andorite; 14, water.

metal-bearing fluids is marked by a dashed line. The proposed path falls into two stages, each with different values of $\Delta \log a_{S_2}/\Delta T$. The first stage, starting from 503 K and 4.5 kbar (the beginning of formation of gudmundite with pyrrhotine) illustrates only the formation of those minerals of which the constituents are the most abundant in a chloride complex solution precipitating sphalerite, gudmundite, and galena (with strong S consumption). Liberated chloride anions are favourable for stronger complexing of the remaining cations so that further diminution of complex stabilities causes deposition of the succeeding minerals. The first stage illustrates rather slow cooling and a relatively steep drop of $\log a_{S_2}$ which is favourable for the formation of simple sulphides. The second stage is characterized by an insignificant fall in $\log a_{S_2}$ and larger changes of temperature and pressure, leading to sulphosalt formation (with strong Sb consumption). In nature, a considerable degradation of weaker chloride complexes would be expected due to a sudden cooling, a drop of pressure, a pH rise, or a fall of transport velocity. Such processes could take place due to contact of the solution with the carbonate rocks, which could bring about a fall in temperature, a rise in pH, and a lower transport velocity owing to lack of textural discontinuities and fissures (e.g. as in the eastern sector carbonates). Considerable complex dissociation and mineral deposition due to a drop of temperature and pressure is also possible when the transporting solution meets an open fissure system at rocks with distinct schistosity as in the western sector hälleflintas and slates.

The tetrahedrite stability field is where the two formation stages cross and this mineral has been observed in the eastern (Ag-poor) and in the western (Ag-richer) parts of the mining district. The analysis of fig. 2 points to the following order of precipitation during the second stage: tetrahedrite → meneghinite → (bournonite) → freibergite → freieslebenite → polybasite → boulangerite → diaphorite → andorite → miargyrite → pyrargyrite → stephanite; corresponding to the systems: (Cu,Ag)-(Fe,Zn)-Sb-S → Cu-Pb-Sb-S → Pb-Sb-S → Pb-Ag-Sb-S → Ag-Sb-S. The presence of meneghinite and bournonite was microscopically confirmed although polybasite was not found. Generally the above succession is similar to that proposed by Nugteren (1978). In considering the formation of silver minerals, the increase in Ag-contents in the lower-temperature minerals such as miargyrite, pyrargyrite and stephanite is interesting. Rather small amounts of stephanite could be explained both by a considerable decrease of Ag content in the solution at the stage of pyrargyrite precipitation (the most abundant Ag-Sb-S mineral) and by the proximity to the Sb/Sb_2S_3 line across which formation of stephanite is quite different and demands much higher $\log a_{S_2}$ (Table I).

In the eastern part of the mining district, the mineralization in borehole samples resembles the distribution which would occur on passing a solution through an adsorption column with adsorbants of varying porosity and pH. In boreholes BH-50, 53, and 51, the first strongly mineralized zone is found in the upper part of the black carbonate sequence. Below this is a section of lower concentrations of ore minerals or a metal-poor transition layer followed by a second enriched zone (fig. 3). In the transition layer, the poorest ore

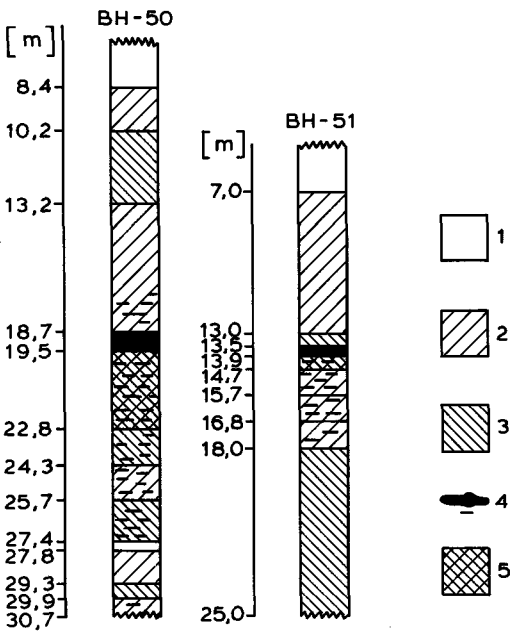

FIG. 3. Schematic section of boreholes 50 and 51 (scale 1:200) 1-cover, 2-hälleflinta, 3-limestone, 4-Pb-Zn-Ag-ore, 5-carbonate.

concentrations occur in the hälleflintas. Abundant examples of pyrargyrite and the earliest high-temperature minerals (arsenopyrite, sphalerite and galena) occur in lower parts of the boreholes. A westwards increase in the concentrations of Pb and Ag (but not Zn) may be a consequence of the varying mobilities of these elements. This is illustrated by a comparison of their amounts in the first strongly mineralized zone (Table II). There is a noticeable westwards rise in the Ag/Pb value suggesting an enrichment in Ag in the western part. The lower value of the Pb concentration in BH-50 compared to BH-53 and BH-51 is caused by the

TABLE II. *Element contents and Ag/Pb values for the first enriched zone in boreholes from the Hällefors deposit*

element %	west ←	borehole	→ east
Ag/Pb	BH-53	BH-50	BH-51
Ag	0.0729	0.0450	0.0186
Pb	7.32	5.78	6.56
Zn	4.84	5.64	20.00
$Ag/Pb \cdot 10^3$	9.96	7.78	2.83

presence of a second enriched zone, non-existent in BH-51.

In the western part of the district, where the mineralization occurs as veins filling fissures and textural discontinuities in slates and hälleflintas, a dominance of the earliest minerals (FeAsS,PbS, ZnS,FeS_2) and some more mobile sulphosalts (from the Ag-Sb-S and Pb-Sb-S systems) is observed. Also notable are occurrences of the small Ag-bearing phases which have an affinity with galena. Analysing phase relations in the system Ag_2S-PbS-Sb_2S_3, Hoda and Chang (1975) point out that andorite forms a rather large stability field and can coexist with almost all other Pb and Pb-Ag sulphantimonides at 573 K.

In Table III, the element contents and some important element ratios in minerals from the Hällefors deposit are arranged in order of formation. This information is also shown graphically in figs. 4 and 5. Similarities between the Sb and S concentration trends point to the similar roles of these elements in the formation of sulphosalts. Figs. 4 and 5 also point to a general decrease in the Sb and S contents and an increase in Ag during the ore-forming process. Also, two stages of Ag deposition are clearly seen. The first consists of minerals from the Cu,Ag)-(Fe,Zn)-Sb-S system, the second comprises the Ag-Sb-S minerals. Pb-Ag-Sb-S minerals could form a link between the two stages. Table III and fig. 5 also illustrate the rise of the Ag/Pb value towards the second stage and the overall sequence of formation of iron → copper → lead → silver phases.

Conclusions. Previous work (Zakrzewski, 1982; Oen *et al.*, 1982) has suggested that the Ag-bearing Hällefors deposits were probably formed by the action of metamorphic solutions on sediments of volcano-sedimentary origin. Carbonates, especially the black carbonates, appear to have acted as collectors of the metal compounds. The ore material was transported from the east to the west along a decreasing pressure gradient and the neighbouring granitic complex may well have acted as an additional source of heat. It seems that the eastern part of the mining district was formed a little earlier and could be treated as one of the sources of ore materials for the western part. Geological and microscopic observations and the analysis of the $\log a_{S_2} - 1/T$ diagram confirm a westwards increase of Ag and Pb concentrations, probably arising from their rather high mobility.

At the stages of sulphosalt and sulphide formation in the deposits, temperature and pressure conditions were probably in the ranges 500-440 K and 4.5-3.5 kbar (fluid inclusion studies). The gudmundite-tetrahedrite stage of this formation process probably occurred in the 500-470 K and 4.5-4.0 kbar ranges and the tetrahedrite-stephanite stage in the ranges 470-440 K and 4.0-3.5 kbar. In agreement with microscopic observations, phase diagrams and thermodynamic calculations, the succession of the Ag-bearing minerals is as follows:

(A) allargentum and dyscrasite as exsolution bodies in Ag-containing galena.

(B) Ag-bearing tetrahedrite → freibergite → miargyrite → pyrargyrite → stephanite (from hydrothermal solutions).

Silver deposition from solution occurs in two

TABLE III. *Element contents and element ratios for some existing and predicted minerals in the Hällefors deposits*

Mineral	Formula	Cu	Sb	S	Pb	Ag	Fe	Ag/Sb+S	Ag/Pb
Tetrahedrite	$Cu_{10}Fe_2Sb_4S_{13}$	38.49	29.50	25.25	—	—	6.77	—	—
Freibergite	$Cu_4Ag_6Fe_{1.5}Zn_{0.5}Sb_4S_{13}$	13.23	25.34	21.69	—	33.68	4.36 (Fe) 4.7 (Zn)	0.72	—
Freieslebenite	$AgPbSbS_3$	—	22.84	18.05	38.87	20.24	—	0.49	0.52
Polybasite	$Ag_{16}Sb_2S_{11}$	—	10.49	15.19	—	74.32	—	2.89	—
Boulangerite	$Pb_5Sb_4S_{11}$	—	25.96	18.80	55.23	—	—	—	—
Diaphorite	$Ag_3Pb_2Sb_3S_8$	—	26.86	18.86	30.47	23.80	—	0.52	0.78
Andorite	$AgPbSb_3S_6$	—	41.85	22.04	23.74	12.35	—	0.19	0.52
Miargyrite	$AgSbS_2$	—	41.45	21.83	—	36.72	—	0.58	—
Pyrargyrite	Ag_3SbS_3	—	22.48	17.76	—	59.76	—	1.48	—
Stephanite	Ag_5SbS_4	—	15.42	16.25	—	68.33	—	2.16	—

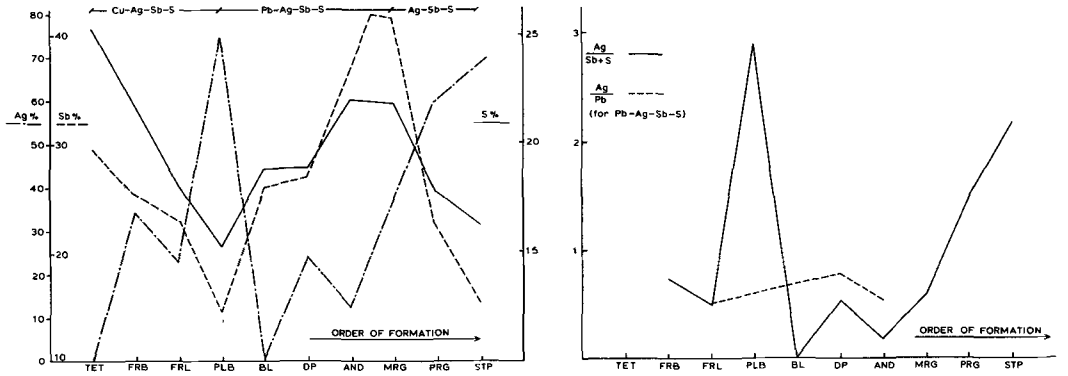

FIGS. 4 and 5. FIG. 4 (*left*). S, Sb, and Ag concentrations in some existing and predicted minerals at Hällefors arranged in order of formation. TET-tetrahedrite, FRB-freibergite, FRL-freieslebenite, PLB-polybasite, BL-boulangerite, DP-diaphorite, AND-andorite, MRG-miargyrite, PRG-pyrargyrite, STP-stephanite. FIG. 5 (*right*). Ag/(Sb+S), Ag/Pb values for some existing and predicted minerals at Hällefors arranged in order of formation (abbreviations as in fig. 4).

substages. The first one is terminated by Ag-rich freibergite, the second involves miargyrite, pyrargyrite, and stephanite with a distinct maximum of precipitation for pyrargyrite. Although, thermodynamically, the coexistence of Pb,Ag,Sb,S-containing minerals with galena and boulangerite is to be expected, they were not observed. Their predicted position in the mineral paragenesis is between the freibergite and miargyrite lines on the $\log a_{S_2} - 1/T$ diagram.

Acknowledgements. I would like to thank Drs D. J. Vaughan, H. Colley, M. A. Zakrzewski, and E. A. J. Burke for critical reading of the manuscript and for valuable suggestions.

REFERENCES

Amcoff, O. (1976) *Neues Jahrb. Mineral. Mh.* 247–61.

Craig, J. R., and Barton, P. B. (1973) *Econ. Geol.* **68,** 493–506.

——and Lees, W. R. (1972) Ibid. **67,** 373–7.

Hall, W. E., and Czamanske, G. K. (1972) *Econ. Geol.* **67,** 350–61.

Hoda, S. N., and Chang, L. L. Y. (1975) *Am. Mineral.* **60,** 621–33.

Jasinski, A. W. (in prep.) *Selected problems of the copper mineralization in the Hällefors region (Bergslagen, Sweden).*

Kostov, I., and Minceva-Stefanova, J. (1981) *Sulphide minerals: crystal chemistry, paragenesis and systematics.* Sofia, 212 pp.

Moorman, A. C., Andriessen, P. A. M., Boelrijk, N. A. I. M., Hebeda, E. H., Oen, I. S., Priem, H. N. A., Verdurmen, E. A. T., Verschure, R. H., and Wiklander, U. (1982) *Geol. För. Förh.* (in press).

Nugteren, H. W. (1978) *The silver mines of Hällefors, Central Sweden.* M.Sc. thesis, Free University of Amsterdam.

——and Zakrzewski, M. A. (in prep.) *The origin and mineralogy of distal volcanosedimentary deposit of Hällefors mine, Bergslagen, Central Sweden.*

Oen, I. S., Helmers, H., Verschure, R. H., and Wiklander, U. (1982) *Geol. Rund.* **71,** 182–94.

Petruk, W., Harris, D. C., Cabri, L. J., and Stewart, J. M. (1971) *Can. Mineral.* **11,** 187–96.

Powell, R. (1978) *Equilibrium thermodynamics in petrology,* Harper and Row, 284 pp.

Robie, R. A., Hemingway, B. S., and Fisher, J. R. (1978) *U.S. Geol. Survey Bull.* 1452, 456 pp.

Sundius, N. (1923) *Sveriges Geol. Undersökning,* ser. C, 312.

——Parwel, A., and Rajandi, B. (1966) Ibid. no. 614.

Tegengren, F. (1924) Ibid. ser. Ca, no. 17.

Welin, E., Wiklander, U., and Kähr, A. M. (1980) *Geol. För. Förh.* **102,** 269–72.

Zakrzewski, M. A. (1982) *Geol. Rund.* **71,** 195–205.

[*Revised manuscript received 14 June 1983*]